ISSN 2176-5480

22nd International Congress of Mechanical Engineering (COBEM 2013)
November 3-7, 2013, Ribeirão Preto, SP, Brazil

NUMERICAL STUDY OF GAS-SOLID DRAG MODELS IN A BUBBLING FLUIDIZED BED

Flávia Zinani
Caterina Gonçalves Philippsen
Maria Luiza Sperb Indrusiak
Mechanical Engineering Graduate Program, Universidade do Vale do Rio dos Sinos – UNISINOS
Av. Unisinos, 950, CEP 93022-000, São Leopoldo, RS, Brazil
fzinani@unisinos.br
catigp@yahoo.com.br
mlsperb@unisinos.br

Abstract. *Bubbling fluidized beds find application mainly in power conversion industries. For design, dimensioning and operation of fluidized bed equipment, the understanding of multiphase gas-solid flows is of great importance. The use of Computational Fluid Dynamics in the simulation of gas-solid systems is limited by the complexity of mathematical models, which rely on a series of empirical or theoretical correlations. In the present work, the code MFIX was employed to simulate flows in a bubbling fluidized bed and to compare results predicted using different gas-solid drag models. An Eulerian mathematical model was employed, in which gas-solid drag correlations, such as Gidaspow, Hill-Koch-Ladd or Syamlal and O'Brien were applied to model momentum transfer between phases. The results predicted were compared with each other and with experimental results from the literature. It was found that for the models of Gidaspow and Hill-Koch-Ladd mesh independency was hard to achieve, while a coarse mesh could be used with Syamlal and O'Brien model yielding mesh independent results. Gidaspow and Hill-Koch-Ladd models predicted the formation of bubbles with shapes more similar to the experiments, while Syamlal and O'Brien model predicted smaller bubbles. Adjusting the coefficients of Syamlal and O'Brien model after the methodology introduced by these authors in 1987, better results were obtained, reproducing experimental results more accurately and preserving good features even in a relatively coarse mesh.*

Keywords: *Bubbling fluidized bed; Gas-solid drag models; MFIX; Numerical simulations.*

1. INTRODUCTION

A major application of bubbling fluidized beds (BFB) is in power conversion industries. A solid fuel is fluidized by air (or an oxidant gas) while the combustion process occurs. This technology is attractive from the environmental standpoint for it allows the use of combinations of various solid fuels, even those of low quality or high humidity content, such as coal, biomass, district and industrial waste and combinations thereof.

A particular feature of bubbling fluidized beds is the formation of gas bubbles. They are responsible for mixing between gas and solids, gas circulation and temperature stabilization. Thus, it is essential to understand its characteristics and transient behavior. Time averaged variables, such as gas and solids velocities, pressure and void fraction are also of great importance for design and determination of operating conditions. They are crucial to the burning process performance in steady state.

Computational Fluid Dynamics (CFD) has become a powerful tool in the understanding of multiphase flows in a wide range of engineering applications and natural processes. This class of problems presents a variety of possibilities with regard to physical and numerical models. In the present paper, both gas and solid phases are modeled using an Euler-Euler framework. For each phase, a continuity equation and a momentum balance equation are solved. Coupling between phases is done via momentum transfer term, in which drag is the most important phenomenon. The gas-solid drag may be modeled using theoretical or empirical correlations. The focus of the present work is to study the performance of three of the most employed gas-solid drag models.

First is the gas-solid correlation of Gidaspow (1986a), which was developed using an empirical correlaton for packed-bed pressure drop (the Ergun equation, 1952). Gidaspow supplemented this correlation with a drag correlation for low values of the solids volume fractions, using a correlation based on the experimental data of Richardson and Zaki (1954), the model of Wen and Yu (1966).

Second is the correlation developed by Syamlal and O'Brien (1987), who used a correlation for the terminal velocity in fluidized or settling beds, expressed as a function of void fraction and Reynolds number, and converted a terminal velocity correlation in a drag correlation.

Third is the correlation developed by Hill et al. (2001a and 2001b) further modified by Benyahia et al. (2006). Hill et al. (2001) introduced the Hill-Koch-Ladd correlation (HKL) based on data from Lattice-Boltzmann simulations. Benyahia et al. (2006) introduced a modification which turned that drag correlation applicable to the full range of void fractions and Reynolds numbers encountered in fluidized bed simulations. It was done by blending the HKL drag

ISSN 2176-5480

correlation with known limiting forms of the gas-solids drag function such that the blended function is continuous with respect to Reynolds number and void fraction.

Some authors have studied the role played by the drag models in numerical results for BFB. Taghipour et al. (2005) found similar results for the models of Syamlal and O'Brien, Gidaspow and Wen e Yu (1966), regarding time-average bed pressure drop, bed expansion and qualitative gas-solid flow pattern. McKeen and Pugsley (2003) compared four drag models in a bubbling bed of fluid catalitic cracking: Syamlal and O'Brien, Gidaspow, Ergun, and Gibilaro et al. (1985), and found that numerical results differ much from experimental results, especially regarding bed expansion. Lundberg et al. (2008), in the simulation of a BFB, employed five drag models (Syamlal and O'Brien (1987), Gidaspow (1986a), Richardson and Zaki (1954), Hill-Koch-Ladd (2001a and 2001b) and RUC - Representative Unit Cell Model). The authors found that the models of Gidaspow, Hill-Koch-Ladd and RUC presented results (bubbling frequency) closer to the experiments. Behjat et al. (2008), in a study of hydrodynamics and heat transfer in a fluidized bed, found that Syamlal and O'Brien model presented better prediction of bed expansion and gas-solid hydrodynamics than Gidaspow model, while in the prediction of bubble shape, both models presented similar results. Hosseini et al. (2010) state that the drag model is a key parameter in modeling gas-solid flows. They analyzed results predicted using Syamlal and O'Brien, Gidaspow and Arastoopour models, finding that only Arastoopour model predicted results similar to experiments. Recently, Esmaili and Mahinpey (2011) presented a study where eleven drag models were compared. They concluded that Syamlal and O'Brien model is a good choice if it is adjusted using the experimental minimum fluidization velocity and void fraction.

In the present work, the open source CFD code MFIX (Multiphase Flow with Interphase eXchanges) was used to simulate flows in a bubbling fluidized bed. The results were used to investigate the role and performance of gas-solid drag models (Gidaspow, Syamlal and O'Brien, Hill-Koch-Ladd) in the prediction of flow hydrodynamics.

2. MATHEMATICAL MODELING

This section describes the mathematical modeling of the problem addressed in this work, which is the hydrodynamic theory for multiphase flows implemented in the code MFIX. Only the part of the mathematical modeling which was the focus of this study is presented in detail. The remainder of the mathematical model can be accessed on the MFIX documentation (Benyahia et al., 2012 and Syamlal et al., 1993).

In flows of interest in this work, the domain is assumed to be filled with a mixture composed of a gas phase and a particulate solid phase. Each phase is modeled as a continuous medium from an Eulerian frame of reference, mapped throughout the domain by its volume fraction, ε_i, which may vary in time and space. Locally, the volume fractions must sum to one, for the phases are considered as interpenetrating continua. Conservation equations of mass and momentum are established for each phase, as described below.

2.1 Mass balance

A mass balance over a control volume for a phase *i* in a non-reactive multicomponent system with no phase changes results in the continuity equation for each phase *i*:

$$\frac{\partial}{\partial t}\left(\varepsilon_i \rho_i\right) + \nabla \cdot \left(\varepsilon_i \rho_i \mathbf{v}_i\right) = 0 \tag{1}$$

where ρ_i is the mass density of phase *i* as a pure substance, and $\mathbf{v}_i$ is the velocity vector for phase *i*. In the present work, the gas phase is modeled as an ideal gas while the solid phase is modeled with a constant mass density throughout the domain.

2.2 Momentum balance

The equations of momentum balance for gas (*g* subscript) and solid (*s* subscript) phases are given by Eqs. (2) and (3), respectively:

$$\frac{\partial}{\partial t}(\varepsilon_g \rho_g \mathbf{v}_g) + \nabla \cdot (\varepsilon_g \rho_g \mathbf{v}_g \mathbf{v}_g) = -\varepsilon_g \nabla p_g + \nabla \cdot \boldsymbol{\tau}_g + \varepsilon_g \rho_g \mathbf{g} - \mathbf{I}_{gs} \tag{2}$$

$$\frac{\partial}{\partial t}(\varepsilon_s \rho_s \mathbf{v}_s) + \nabla \cdot (\varepsilon_s \rho_s \mathbf{v}_s \mathbf{v}_s) = -\varepsilon_s \nabla p_g + \nabla \cdot \boldsymbol{\tau}_s + \varepsilon_s \rho_s \mathbf{g} + \mathbf{I}_{gs} \tag{3}$$

On the left side of Eqs. (2) and (3), the first term represents the rate of change of momentum and the second term is the advection of momentum. The first and second terms on the right represent the surface forces, the third term

ISSN 2176-5480

represents body forces (eg. gravity, **g**) and the last term represents the momentum transfer between gas and solid phases. In Eqs. (3) and (4), p_g is the gas pressure and $\boldsymbol{\tau}_i$ is the stress tensor of each phase. The gas phase is assumed to behave as a newtonian fluid with constant viscosity, μ_g.

2.3 Gas-solid drag models

The momentum transfer between fluid and solid phases is represented in Eq. (2) and (3) as $\mathbf{I}_{gs}$. In MFIX, only the effects of drag are considered in modeling $\mathbf{I}_{gs}$, for they are usually the most significant in gas-solid multiphase flows (Syamlal et al., 1993). The drag force arises due to velocity differences between the phases, so, $\mathbf{I}_{gs}$ may be represented as the following relation:

$$\mathbf{I}_{gs} = \beta_{gs}(\mathbf{v}_g - \mathbf{v}_s) \tag{4}$$

where β_{gs} is the drag function, which is modeled via empirical or theoretical correlations, i.e., drag models. MFIX offers a list of possible drag models to be used in simulations. In the present work, three drag models were employed: Gidaspow, Syamlal and O'Brien and Hill-Koch-Ladd (HKL). They are described below.

2.3.1 Gidaspow drag correlation

To model the drag function at low values of void fraction ($\varepsilon_g < 0.8$), Gidaspow (1986a) employs the Ergun equation (1952), which is based on pressure-drop data for packed beds. For the disperse phase, Gidaspow employs the Wen-Yu correlation for pressure drop to derive an expression for the drag function:

$$\beta_{gs} = \begin{cases} \dfrac{150\varepsilon_s^2\mu_g}{\varepsilon_g d_p^2} + \dfrac{1.75\rho_g\varepsilon_s}{d_p}\left|\mathbf{v}_g - \mathbf{v}_s\right| & \text{if} \quad \varepsilon_g < 0.8 \\ \dfrac{3}{4}\dfrac{\rho_g\varepsilon_g\varepsilon_s}{d_p}C_D\left|\mathbf{v}_g - \mathbf{v}_s\right|\varepsilon_g^{-2.65} & \text{if} \quad \varepsilon_g \geq 0.8 \end{cases} \tag{5}$$

where μ_g is the gas viscosity, d_p is the mean particle diameter and $\left|\mathbf{v}_g - \mathbf{v}_s\right|$ is the magnitude of the relative velocity between gas and solid phases. The drag coefficient, C_D, is related to the Reynolds number after Rowe (1961):

$$C_D = \begin{cases} \dfrac{24}{Re_G}(1 + 0.15Re_G^{0.687}) & \text{if} \quad Re < 1000 \\ 0.44 & \text{if} \quad Re \geq 1000 \end{cases} \tag{6}$$

with the model's Reynolds number given as

$$Re_G = \frac{\rho_g\varepsilon_g\left|\mathbf{v}_g - \mathbf{v}_s\right|d_p}{\mu_g} \tag{7}$$

2.3.2 Syamlal and O'Brien drag correlation

The Syamlal and O'Brien drag correlation (1987) employs β_{gs} as a function of a drag coefficient:

$$\beta_{gs} = \frac{3}{4}\frac{\rho_g\varepsilon_g\varepsilon_s}{d_p}C_D\left|\mathbf{v}_g - \mathbf{v}_s\right| \tag{8}$$

where C_D is a function of the particle Reynolds number, Re_{SO}, and the void fraction, ε_g. The model's Reynods number is given by

$$Re_{SO} = \frac{\rho_g\left|\mathbf{v}_g - \mathbf{v}_s\right|d_p}{\mu_g} \tag{9}$$

ISSN 2176-5480

Syamlal and O'Brien employ a correlation proposed by Garside and Al-Dibouni (1977) to calculate C_D:

$$C_D = \left[\frac{0.63}{V_r} + \frac{4.8}{\left(V_r Re_{SO}\right)^{1/2}} \right]^2 \tag{10}$$

where the ratio of the terminal settling velocity of a multiparticle system to that of an isolated single particle, V_r, is calculated as follows:

$$V_r = 0.5\left(\varepsilon_g^{4.14} - 0.06 Re_{SO} + \sqrt{\left(0.06 Re_{SO}\right)^2 + 0.12 Re_{SO}\left(2B - \varepsilon_g^{4.14}\right) + \varepsilon_g^{8.28}} \right) \tag{11}$$

with coefficient B given as:

$$B = \begin{cases} 0.8\varepsilon_g^{1.28} & \text{if} \quad \varepsilon_g \le 0.85 \\ \varepsilon_g^{2.65} & \text{if} \quad \varepsilon_g > 0.85 \end{cases} \tag{12}$$

2.3.3 Hill-Koch-Ladd drag correlation

The Hill-Koch-Ladd drag correlation is based on numerical results for the drag exerted by a fluid flow on a collection of ramdomly dispersed fixed particles. Such calculations were performed using the Lattice-Boltzmann Method, which is based on fundamental principles in mechanics. Hill et al. (2001a and 2001b) performed calculations over a range of Reynolds numbers and void fractions, and reported a functional representation which was precisely fit to this data, obtaining different formulas applicable to different ranges of Reynolds number and void fraction. Benyahia (2006) modified the Hill-Koch-Ladd (HKL) formulas to span a full range of the Re-ε_g space. With the drag function given as in Eq. 9, C_D in the modified HKL correlation is given as:

$$C_D = \frac{12(1-\varepsilon_s)^2}{Re_{HKL}} F \tag{13}$$

where the drag force F is given by:

$$F = \begin{cases} 1 + 3/8\, Re_{HKL} & \text{if} \quad \varepsilon_s \le 0.01 \quad \text{and} \quad Re_{HKL} \le \dfrac{\left(F_2 - 1\right)}{\left(3/8 - F_3\right)} \\ F_0 + F_1 Re_{HKL}^2 & \text{if} \quad \varepsilon_s > 0.01 \quad \text{and} \quad Re_{HKL} \le \dfrac{F_3 + \left[F_3^2 - 4F_1\left(F_0 - F_2\right)\right]^{0.5}}{2F_1} \\ F_2 + F_3 Re_{HKL} & \text{if} \quad \varepsilon_s \le 0.01 \quad \text{and} \quad Re_{HKL} > \dfrac{\left(F_2 - 1\right)}{\left(3/8 - F_3\right)} \quad \text{or} \quad \varepsilon_s > 0.01 \quad \text{and} \quad Re_{HKL} > \dfrac{F_3 + \left[F_3^2 - 4F_1\left(F_0 - F_2\right)\right]^{0.5}}{2F_1} \end{cases} \tag{14}$$

with coefficients and model's Reynolds number calculated as follows:

$$F_0 = \begin{cases} \left(1-w\right)\left[\dfrac{1 + 3\left(\varepsilon_s/2\right)^{0.5} + \left(135/64\right)\varepsilon_s \ln\left(\varepsilon_s\right) + 17.14\varepsilon_s}{1 + 0.681\varepsilon_s - 8.4\varepsilon_s^2 + 8.16\varepsilon_s^3} \right] + w\left[10\dfrac{\varepsilon_s}{\left(1-\varepsilon_s\right)^3} \right] & \text{if} \quad 0.01 < \varepsilon_s < 0.4 \\ 10\dfrac{\varepsilon_s}{\left(1-\varepsilon_s\right)^3} & \text{if} \quad \varepsilon_s \ge 0.4 \end{cases} \tag{15}$$

$$F_1 = \begin{cases} \left(2/\varepsilon_s\right)^{0.5}/40 & \text{if} \quad 0.01 < \varepsilon_s \le 0.1 \\ 0.11 + 0.00051\exp(11.6\varepsilon_s) & \text{if} \quad \varepsilon_s > 0.1 \end{cases} \tag{16}$$

ISSN 2176-5480

$$F_2 = \begin{cases} (1-w)\left[\dfrac{1+3(\varepsilon_s/2)^{0.5}+(135/64)\varepsilon_s\ln(\varepsilon_s)+17.89\varepsilon_s}{1+0.681\varepsilon_s-11.03\varepsilon_s^2+15.41\varepsilon_s^3}\right]+w\left[10\dfrac{\varepsilon_s}{(1-\varepsilon_s)^3}\right] & \text{if} \quad \varepsilon_s < 0.4 \\ 10\dfrac{\varepsilon_s}{(1-\varepsilon_s)^3} & \text{if} \quad \varepsilon_s \geq 0.4 \end{cases} \tag{17}$$

$$F_3 = \begin{cases} 0.9351\varepsilon_s + 0.03667 & \text{if} \quad \varepsilon_s < 0.0953 \\ 0.0673 + 0.212\varepsilon_s + 0.0232/(1-\varepsilon_s)^5 & \text{if} \quad \varepsilon_s \geq 0.0953 \end{cases} \tag{18}$$

$$Re_{HKL} = \frac{\rho_g \varepsilon_g \left|\mathbf{v}_g - \mathbf{v}_s\right| d_p}{2\mu_g} \tag{19}$$

$$w = \exp\left(-10(0.4-\varepsilon_s)/\varepsilon_s\right) \tag{20}$$

2.4 Turbulence models and solid phase stress tensor

In MFIX, to model the solid phase stress tensor, the theories for plastic and viscous regimes are combined using a critical void fraction (usually the minimum fluidization void fraction, $\varepsilon_{g,mf}$) in which a transition from viscous to plastic regime occurs. A modified Princeton model based on the Kinetic Theory for Granular Flows is used to model the solid phase stress tensor in viscous regime (Benyahia et al., 2012). For the plastic regime, the Schaeffer frictional stress model is employed (Benyahia et al., 2012, Schaeffer, 1987). The gas-solids turbulence models implemented in MFIX are described in detail in Benyahia et al. (2005). The k-ε model is used to model gas turbulent kinetic energy and gas turbulent dissipation, while the Simonin model with the partial differential equation for the granular temperature is used to model solids turbulence. For the radial distribution function, the Carnahan-Starling model is used.

3. PROBLEM STATEMENT

The geometry of the BFB reactor used in all numerical tests is a classical test based on the work of Gidaspow et al. (1983), and also described by Gidaspow (1994), and depicted schematically in Fig. 1. It consists of a two-dimensional geometry, with height L = 0.5844 m and width W = 0.3937 m. Air ($\mu_g = 1.8 \cdot 10^{-4}$ Pa s, M_g = 29 g/mol) is injected from a central jet 0.0127 m wide at velocity, $v_{g,jet}$, equal to 3.55 m/s. Air is also blowed uniformly from the bottom of the geometry at 0.284 m/s, the minimum fluidization velocity. At the initial condition, particles fill the geometry up to 0.2922 m while air flows with superficial vertical velocity of 0.284 m/s throughout the particulate bed, maintaining it at a minimum fluidization condition, with the minimum fluidization void fraction, $\varepsilon_{g,mf}$ equal to 0.44. The mean particle diameter, d_p, is of $5 \cdot 10^{-4}$ m, the solids mass density, ρ_s, is of 2610 kg/m^3 and restitution coefficient, e, equal to 0.8. The outlet pressure is 101 kPa. The total time of simulation was 40 s. It was assumed that steady state was achieved when the time averaged solids volume fraction at the center of the reactor achieved a constant value. For the three drag models employed, this was achieved before 20 s, so the time average results presented herein are calculated between 20 and 40 s.

ISSN 2176-5480

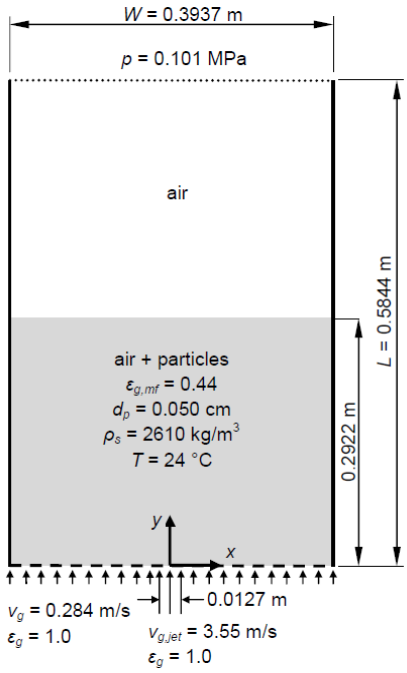

Figure 1: Problem statement

4. RESULTS AND DISCUSSION

4.1 Grid study and comparison with experimental results

A grid study was performed in order to analyze the dependency of the results for each of the models employed on the grid refinement. The grids consisted of 124 x 108 (G1), 186 x 162 (G2), 248 x 216 (G3) and 310 x 270 (G4) control volumes in the directions x and y, respectively.

The results were compared with experimental results of Gidaspow et al. (1983) for the time averaged solids volume fraction at the centerline, along the dimensionless vertical position, $y^* = y/L$. These results are depicted in Fig. 2 for (a) Gidaspow, (b) Syamlal and O'Brien and (c) HKL drag models.

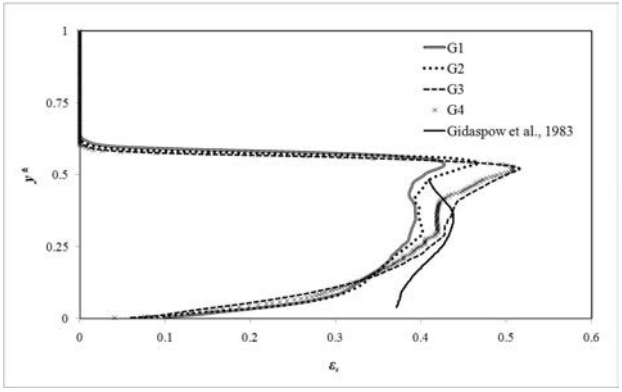

(a)

ISSN 2176-5480

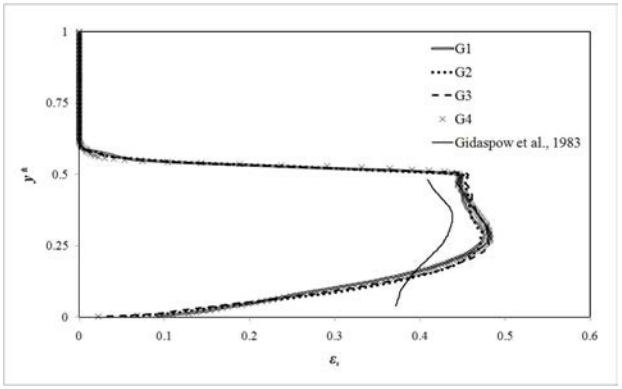

(b)

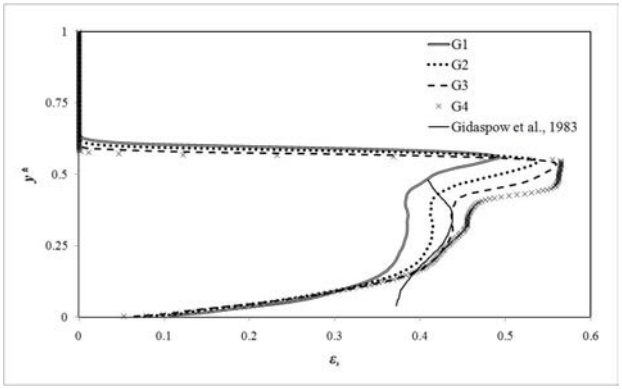

(c)

Figure 2: Time averaged solids volume fraction at the centerline. (a) Gidaspow, (b) Syamlal and O'Brien and (c) HKL drag models.

The three drag models underestimate the value of ε_s at low values of y^* due to the imposition of the boundary condition of $\varepsilon_s = 0$ at $y^* = 0$.

When Gidaspow model is employed (Fig 2.a), there is a considerable change in results when the grid is refined from G2 to G3. The finest grid predicts higher values of ε_s along the centerline, indicating that the bubbles divide and burst at a lower position. For the Syamlal and O'Brien model (Fig. 2.b), the grid refinement does not promote a considerable change in the results. However, the ε_s profile is farther from experimental results than that predicted by Gidaspow model. Using the HKL model, there is also a tendency to predict higher ε_s when the grid is refined.

The following results were obtained using grid G3, for the differences between G3 and G4 results for the ε_s profile were of less than 10% for all models.

4.2 Bubble formation

Bubble formation is an important factor in BFB operation, because it influences the mixture between phases, the bed expansion and the elutriation process, in which smaller particles are separated from larger particles. The upward movement of the bubbles promotes mixing between the phases and, consequently, improves heat and mass transfer. The bed expansion is influenced by the volume of bubbles, and elutriation is influenced by the collapse of bubbles on the surface of the bed due to the release of particles in the freeboard area. So, the correct prediction of bubble formation is an essencial parameter in numerical simulation.

The average bubble sizes were analyzed via time averaged void fraction profile at two vertical positions, $y^* = 0.25$ (Fig. 3a) and $y^* = 0.5$ (Fig. 3b). The dimensionless position is given by $x^* = 2x/W$. The void fraction profile at $y^* = 0.25$ shows that the bubbles predicted using Gidaspow and HKL models have greater diameter. This is the region where the bubbles have not splitted yet. At $y^* = 0.5$, the void fraction profile suggests that the bubbles split in two and form two pronounced void fraction peaks for the Gidaspow and HKL models. For the Syamlal and O'Brien model, the void fraction profile is more uniform, because the bubbles formed using this model colapse at the center of the reactor, and promote a lower bed expansion, causing higher values of void fraction at this position.

ISSN 2176-5480

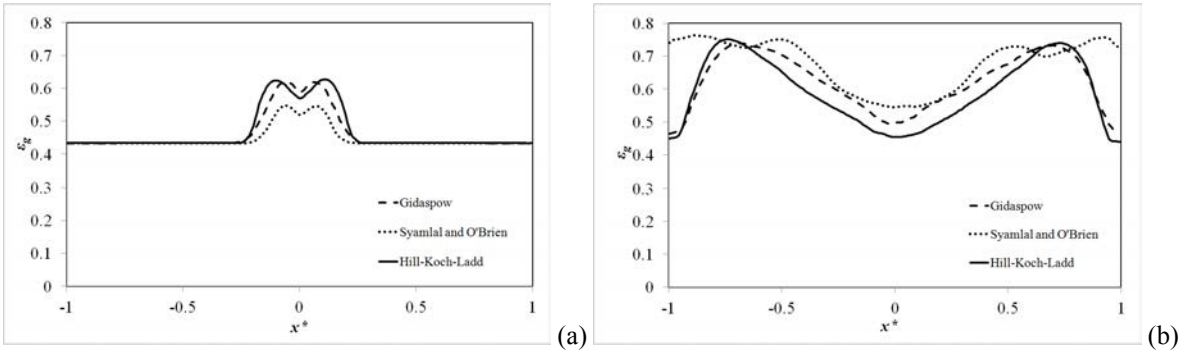

Figure 3: Time average void fraction at: (a) $y^* = 0.25$ and (b) $y^* = 0.5$.

Figure 4 depicts typical bubble shapes predicted by the three drag models. These pictures were taken at 30 s of simulations, using the data visualizer software Paraview.

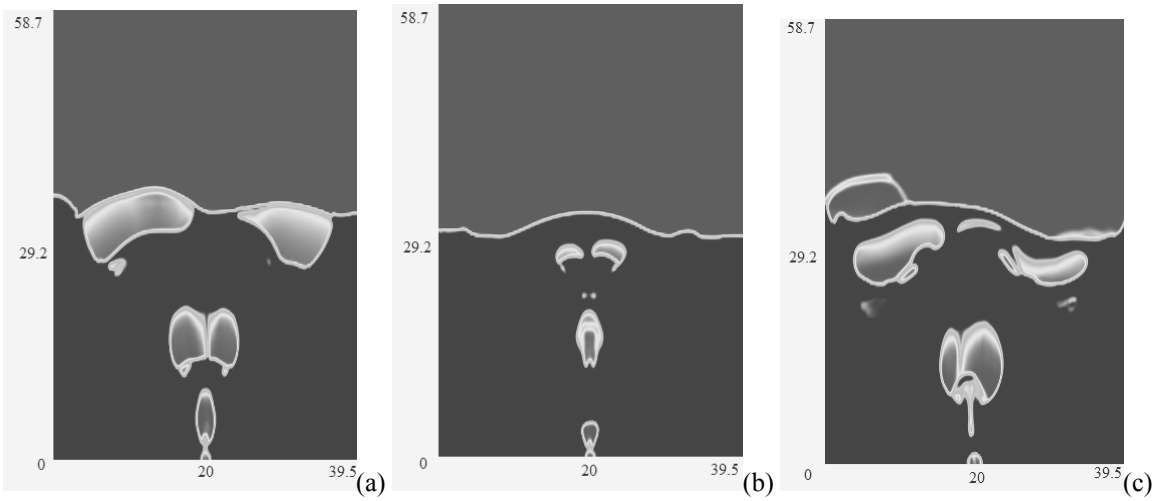

Figure 4:Typical bubble shapes predicted by (a) Gidaspow, (b) Syamlal and O'Brien and (c) HKL drag models

While Gidaspow and HKL models predict bubbles with similar shape and diameter, Syamlal and O'Brien's model predicts bubbles of much smaller diameter. Using Gidaspow and HKL models, when the bubbles separate from the jet and afterwards divide in two parts, they start to occupy the whole bed region, and collapse near the walls. With Syamlal and O'Brien model, the small bubbles separate and divide, but collapse at the middle region of the bed.

Figure 5 is a comparison of the bubble shape predicted by the three models and the experimental result by Gidaspow et al. (1986b), which employed similar conditions. All results are for the instant of 0.32 s. It is possible to observe that Gidaspow and HKL models predict bubble shapes more similar to the experimental results.

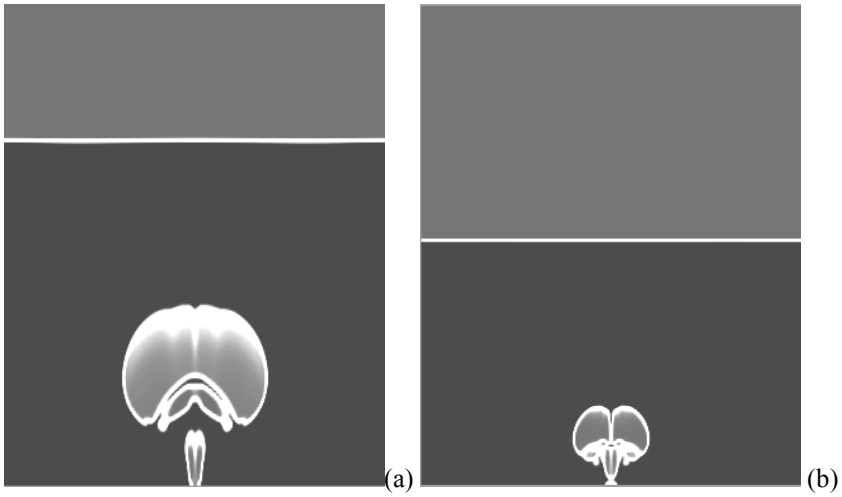

ISSN 2176-5480

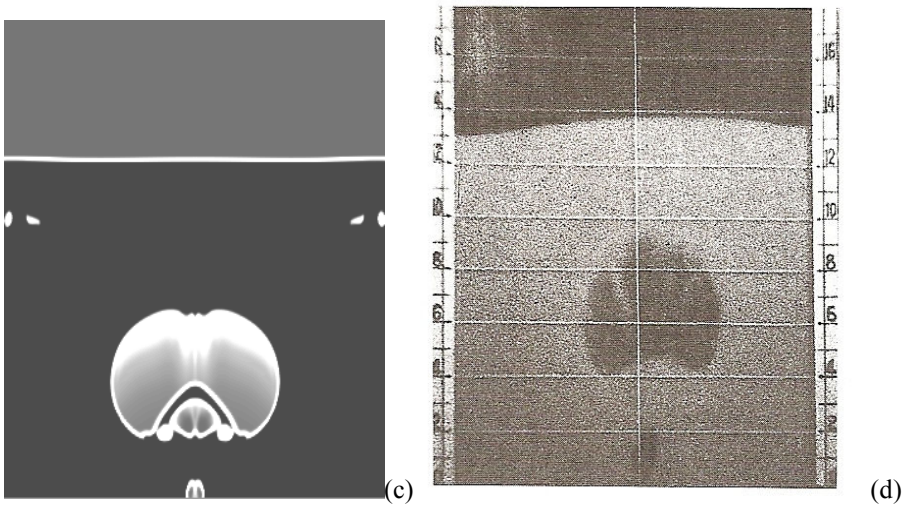

(c) (d)

Figure 5: Bubble shapes at 0.32 s predicted by drag models of (a) Gidaspow, (b) Syamlal and O'Brien and (c) HKL and (d) experimental results by Gidaspow (1986b)

The distinct behavior predicted by Syamlal and O'Brien model might be due to the model parameters employed in Eq. 12. This equation is the original drag law introduced by Syamlal and O'Brien (1987). However, it has been shown that it predicts a higher minimum fluidization velocity than experiments (Esmaili and Mahinpey, 2011). In this case, the jet velocity would not be enough to generate large bubbles as the experiment shows.

4.3 Time averaged void fraction

The time averaged void fraction fields obtained using the three drag models are depicted in Fig. 6, where the color scale represents the void fraction scale. The darkest color corresponds to $\varepsilon_g = 0.44$ and the lightest color corresponds to $\varepsilon_g = 1$.

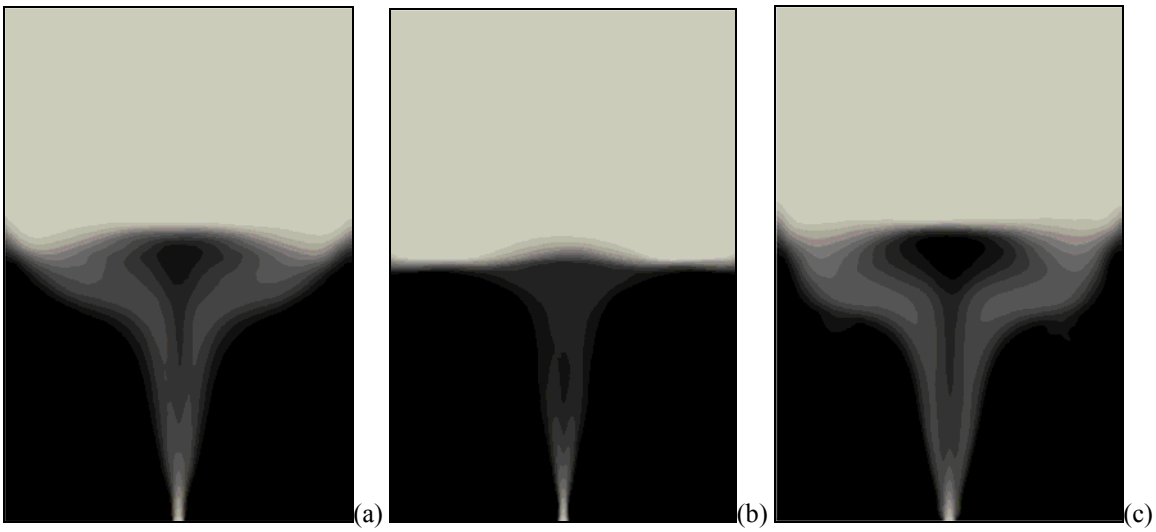

(a) (b) (c)

Figure 6: Time averaged void fraction field. (a) Gidaspow, (b) Syamlal and O'Brien and (c) HKL drag models.

In Fig. 6, the path followed by the bubbles during the experiment is tracked by the region of high ε_g at the vertical centerline of the bed. Also, bubble division is tracked by the formation of a region of low ε_g at the center of geometry. The HKL model predicts a pronounced region of low ε_g at the center of geometry, meaning that a bubble division is happening just below that region, and that the bubbles get to the free board far from the centerline. Gidaspow model predicts a similar result, but with a smaller region of low ε_g, meaning that the bubbles get to the free board farther from the walls than with HKL model. Also, the bed expansion predicted by HKL model is the largest one. Syamlal and O'Brien model predicts the smallest bed expansion, and also the smallest region through which the bubbles travel, meaning that the bubbles might not experiment a division and thus get to the free board as single bubbles. A link

ISSN 2176-5480

between results shown in Fig. 2 and 6 can be made. The high value of solids volume fraction predicted by Gidaspow and HKL models shown in Fig. 2 is translated as the region of low ε_g at the center of geometry in Fig. 6.

4.4 Time averaged gas velocity

Figure 7 shows the time averaged gas velocity vectors predicted by the three drag models. All models predict higher velocities near the walls in the free board. Syamlal and O'Brien (Fig. 7a) predicts a more uniform velocity field along the bed, while Gidaspow (Fig. 7b) and HKL (Fig. 7c) predict a higher velocity in the jet region. The HKL model even predicts the formation of recirculation zones at the bed, along the walls.

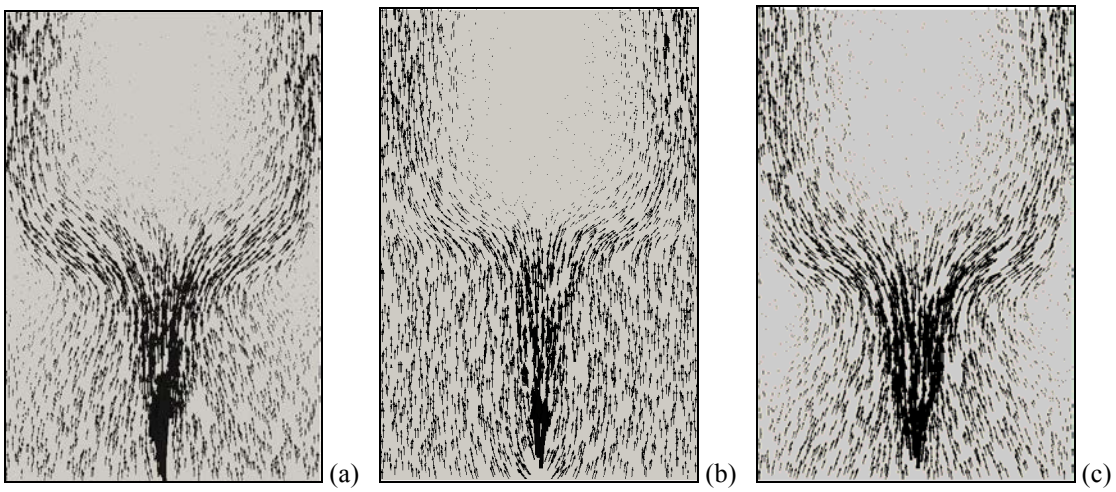

Figure 7: Time averaged gas velocity vectors. (a) Gidaspow, (b) Syamlal and O'Brien and (c) HKL drag models.

5. FINAL REMARKS

The gas-solid drag models of Gidaspow, Syamlal and O'Brien and Hill-Koch-Ladd were employed in the numerical simulation of a bubbling fluidized bed with a central jet. It has been shown that the gas-solid drag model is a key feature in the mathematical modeling of multiphase flows in bubbling fluidized beds, for the choice of a specific model affects drastically instantaneous and time averaged results. For the same initial and boundary conditions, Syamlal and O'Brien model achieved better grid convergence and predicted the formation of smaller bubbles than Gidaspow and HKL models, in this way predicting a more uniform flow along the reactor. Using Gidaspow and HKL models, bubbles with higher diameter were predicted, which tended to divide and burst along the the bed surface, promoting higher mixture and formation of recirculation zones near the walls. Also, Gidaspow and HKL drag models predicted bubble shapes more similar to experimental results. The difficulty of Syamlal and O'Brien model to predict experimental results might be due to a bad choice of model parameters, which are not adjusted to predicct experimental minimum fluidization velocity. This is a question for further work. In the present work, the comparison of numerical results with experimental ones helped the choice of the best suited drag model for the representation of the actual process. Experiments using a wider range of parameters might be a promising tool for further adjustment of gas-solid drag correlations.

6. ACKNOWLEDGEMENTS

The authors acknowledge CNPq for the financial support through grants PQ2/2011-2013 and DTI/2010-2011.

7. REFERENCES

Behjat, Y., Shahhosseini, S., Hashemabadi, S.H., 2008. CFD modeling of hydrodynamic and heat transfer in fluidized bed reactors. **Int. Commun. Heat Mass** v. 35, p. 357–368.

Benyahia S., 2005. **Gas/Solid Turbulence Models Implemented in MFIX**. From URL https://mfix.netl.doe.gov/documentation/Simonin_Ahmadi_Models.pdf.

Benyahia, S., Syamlal, M, O'Brien, T.J., 2006. Extension of Hill Koch Ladd drag correlation over all ranges of Reynolds number and solids volume fractions. **Powder Technology**, v. 162, p. 166-174.

Benyahia, S., Syamlal, M., O'Brien, T.J., 2012. **Summary of MFIX Equations 2012-1**, From URL https://mfix.netl.doe.gov/documentation/MFIXEquations2012-1.pdf.

Ergun, S., 1952. Fluid flow through packed columns. **Chem. Eng. Prog**. v. 48, p. 89–94.

ISSN 2176-5480

Esmaili, E., Mahinpey, N., 2011. Adjustment of drag coefficient correlations in three dimensional CFD simulation of gas–solid bubbling fluidized bed. **Advances in Engineering Software**, v. 42, p. 375–386.

Garside, J., Al-Dibouni, M.R., 1977. Velocity–voidage relationships for fluidization and sedimentation in solid–liquid systems. **Industrial Engineering Chemistry: Process Design and Development**. v. 16, p. 206–214.

Gibilaro, L.G., Di Felice, R., Waldron, S.P, Foscolo, P.U., 1985. Generalized friction factor and drag coefficient correlations for fluid–particle interactions. **Chemical Engineering Science**, v. 40, p. 1817–1823.

Gidaspow, D., 1986a. Hydrodynamics of fluidization and heat transfer: supercomputer modeling. **Appl. Mech. Rev.**, v. 39, p. 1-23.

Gidaspow, D., Syamlal, M., Seo, Y.C., 1986b. Hydrodynamics of fluidization: supercomputer generated vs. experimental bubbles. **J. Powder & Bulk Solids Tech.** v. 10, p. 19-23.

Gidaspow, D., Lin, C., Seo, Y.C., 1983. Fluidization in Two-Dimensional Beds with a Jet. 1. Experimental Porosity Distributions. **Ind. Eng. Chem. Fundam.**, v. 22, p. 187-193.

Gidaspow, D., 1994. **Multiphase Flow and Fluidization – Continuum and Kinetic Theory Descriptions.** Ed. Academic Press, London, 467 p.

Hill, R.J., Koch, D.L., Ladd, J.C., 2001b. Moderate-Reynolds-number flows in ordered and random arrays of spheres. **Journal of Fluid Mechanics**, v. 448, p. 243–278.

Hill, R.J., Koch, D.L., Ladd, J.C., 2001a. The first effects of fluid inertia on flows in ordered and random arrays of spheres. **Journal of Fluid Mechanics**, v. 448, p. 213–241.

Hosseini, S.H., Ahmadi, G., Rahimi, R., Zivdar, M., Esfahany, M.N., 2010. CFD studies of solids hold-up distribution and circulation patterns in gas–solid fluidized beds. **Powder Technology**, v. 200, p. 202–215.

Lundberg, J., Halvorsen, B.M., 2008. A Review of Some Existing Drag Models Describing the Interaction Between Phases in a Bubbling Fluidized Bed. **49th Scandinavian Conference on Simulation and Modeling**.

Mckeen, T., Pugsley, T., 2003. Simulation and experimental validation of a freely bubbling bed of FCC catalyst. **Powder Technology**, v. 129, p. 139–152.

Richardson, J.F., Zaki, W.N., 1954. Sedimentation and Fluidization: Part I. **Trans. Inst., Chem. Eng.**, v. 32, p. 35-53.

Rowe, P.N., 1961. Drag forces in a hydraulic model of a fluidized bed, Part II. **Trans. Inst. Chem. Engs.**, v. 39, p. 175-180.

Schaeffer, D.G. 1987. Instability in the evolution equations describing incompressible granular flow. **Journal of Differential Equations**, v. 66, p. 19–50.

Syamlal, M., . O'Brien, T.J. A, 1987. Generalized drag correlation for multiparticle systems". Morgantown Energy Technology Center DOE Report.

Syamlal, M., Rogers, W., O'Brien, T.J. **MFIX Documentation: theory guide**. DOE Technical note, 1993.

Taghipour, F., Ellis, N., Wong, C., 2005. Experimental and computational study of gas–solid fluidized bed hydrodynamics**. Chemical Engineering Science,** v. 60, p. 6857–6867.

Wen, Y.C., Yu, Y.H., 1966. Mechanics of fluidization**. Chem. Eng. Prog. Symp. Ser**. v. 62, p. 100 – 111.

8. RESPONSIBILITY NOTICE

The authors are the only responsible for the printed material included in this paper.